P12.3

AN OBSERVATIONAL STUDY OF THE INTERACTION BETWEEN A SUPERCELL AND A MESOSCALE BOUNDARY

Mark R. Conder[1]*, Steve Cobb[1], Gary D. Skwira[1], and John L. Schroeder[2],
[1]National Weather Service Forecast Office, Lubbock, Texas
[2]Department of Geosciences, Texas Tech University, Lubbock, Texas

1. INTRODUCTION

This study examines a case of a supercell that interacted with a pre-existing low-level boundary on 5 October 2003. This case is intriguing in that it was a late-season event, the synoptic environment was not particularly favorable for the development of supercell tornadoes, and the event was well sampled by the West Texas Mesonet high-resolution meteorological network of surface stations. The analysis will show that the boundary was responsible for an intensification of the storm mesocyclone and subsequent development of a brief F1 tornado (along with a 85-km swath of severe hail). Numerous previous studies have shown that low-level boundaries may play significant roles in the evolution of supercell storms and development of tornadoes. In the VORTEX-95 experiment, it was noted that the large majority of storms that produced tornadoes did so after interacting with a mesoscale boundary (Markowski et al, 1998). In our case, the boundary was a convergent and baroclinic zone that was caused by a thunderstorm outflow moving westward from previous convection. Convergence was produced by a strong easterly component of the wind on the cool side of the boundary with a southwest wind on the warm side. The baroclinicity along the boundary was reinforced by both the enhancement of the temperature gradient in the convergent flow and differential heating brought about by an extensive area of low clouds to the east of the boundary during the morning hours on 5 October. In this study we utilize surface observations obtained from the West Texas Mesonet (WTXM) to track the boundary at five minute intervals and study the effects it has on the storm evolution as diagnosed by radar imagery from the Lubbock WSR-88D. Our analysis is also aided by a 20 GMT sounding taken from Reese Center.

2. SYNOPTIC AND MESOSCALE ENVIRONMENT

At first glance, the atmospheric environment did not appear particularly conducive for the development of tornadic supercells. The synoptic pattern was characterized by a small shortwave trough moving southeast through the central and high plains states in between a vigorous trough over southeastern Canada/northeastern United States and a broad ridge over the spine of the Rocky Mountains. As can be seen in Figure 1, the mid-level shortwave trough axis was crossing the Texas Panhandle on the morning of the 5th, bringing vorticity and weak cold air advection at 500hPa (Figure 1a). At 850hPa, pronounced warm air and moisture advection was occurring ahead of the trough (Figure 1b), The 850hPa wind itself was fairly weak, following the diurnal phase of the low-level jet. A kinematic analysis of the 250 and 500 hPa levels show that the 250 hPa wind maximum stretched from northeastern New Mexico across the northern Texas Panhandle (Figure 2a). The 500 hPa jet core was located further south, oriented northwest to southeast over the approximate location of the storm development (Figure 2b). However, the wind speed in the jet core was less than 30 knots.

At the mesoscale, Figure 3 shows the satellite imagery and boundary positions at the approximate time of convective initiation (20 GMT). A cluster of thunderstorm cells can be seen developing in an area bounded by the location of the two boundaries and the 5ºC 12 hour^{-1} contour of 850 hPa temperature advection. The storm of interest develops out of this cluster in southern Randall County (indicated on the image). Once the storm had initiated, it moved to the southeast while the outflow boundary (OB) was moving west. According to radar imagery, the storm crossed the OB at approximately 2230 GMT. The environment on the "cool" side of the boundary was markedly different from the "warm" side. The WTXM sounding was modified to take into account the surface observations on either side of the OB. The resulting soundings and hodographs are shown in Figure 4. Some of the pertinent calculations from the soundings are shown in table 1.

Table 1. Sounding derived parameters

Parameter	West	East
LCL	1364 m	611 m
LFC	1878 m	1964 m
s-rH* 0-1 km	46 m^2 s^{-2}	200 m^2 s^{-2}
s-rH* 0-2 km	67 m^2 s^{-2}	219 m^2 s^{-2}
s-rH* 0-3 km	92 m^2 s^{-2}	245 m^2 s^{-2}
Total CAPE	1551 J kg^{-1}	1319 J kg^{-1}
Vorticity generation potential (VGP) 0-4 km	.273 m s^{-2}	.365 m s^{-2}

* Using a storm motion vector of 320/18 kts

* Corresponding author address: Mark R. Conder, National Weather Service, 2579 S. Loop 289, Suite 100, Lubbock, TX 79423-1400
email: mark.conder@noaa.gov

3. STORM/BOUNDARY INTERACTION

The storm and the boundary were tracked using the lowest three elevation tilts (0.5, 1.5 and 2.4 degrees) while in VCP 11 (14 elevations in 5 minutes). In order to characterize the near-storm environment in the vicinity of the OB, the WTXM observations were analyzed utilizing the GEMPAK objective analysis and derived variable calculation schemes. The parameters used in the characterization were absolute vorticity, moisture convergence, equivalent potential temperature (theta-e), and theta-e advection. Prior to the time the storm crossed the boundary, the theta-e analysis shows that storm developed on the nose of a theta-e ridge, and then moved southeast along the east side of the ridge axis (Figure 5). This was also coincided with a region of persistent moisture convergence and cyclonic vorticity (not shown) that contributed to the storm's intensification.

Convergent velocity signatures from the radar data showed that a broad mid-level mesocyclone was developing in the storm. However, the mesocyclone rapidly intensified after interaction with the OB and presumably would not have done so otherwise. The evolution of the storm's mesocyclone was tracked by using rotational velocity (V_r) measurements. These were performed by manually interrogating the radar data using the AWIPS "V_r shear" tool. The results are depicted in Figure 6. This figure shows that the broad 20-30 kt circulation underwent a strengthening at all three levels reaching a maximum of approximately 50 kts at 2300 GMT, just several minutes before the tornado was reported at 2205 GMT. Also in this time frame there was also a decrease in the circulation diameter (not shown). The tornado lasted approximately 15 minutes – until 2320 GMT. Soon thereafter, the low level mesocyclone quickly lost strength while the mid-level mesocyclone was maintained and even strengthened. This is most likely due to the continued westward motion of the OB and the increasing distance between the storm and the axis of vorticity. The representation of the storm in the Radar imagery also shows this evolution. At 2300 GMT, the storm had developed a strong velocity couplet (Figure 7a) and a large hook-like appendage in the reflectivity data (Figure 7b). By 2346 GMT, the storm had largely lost its low level velocity couplet (Figure 8a) but had maintained the strong mid-level rotation as evidenced by the BWER at 1.5 degrees (Figure 8b).

4. CONCLUSIONS

The interaction of the storm on 5 October 2003 with an OB was likely responsible for the storm's intensification and subsequent production of an F1 tornado – approximately 30 minutes after the storm crossed the boundary. The storm relative helicity on the cool side of the boundary was increased by at least a factor of two and became more typical of that associated with strong mesocyclone formation (0-3 km helicity threshold of 150 m^2 s^{-2} given by Davies-Jones and Burgess, 1990). The development and strengthening of the mesocyclone was thus related to tilting of this horizontal streamwise vorticity into vertical vorticity.

Research by Trapp et al (1999) indicates that the type of non-descending tornadogenesis displayed in this case is representative of storms interacting with low-level boundaries. Through utilization of mesoscale observations such as those present on this day, forecasters can consider the modifications of the pre-storm environment by boundaries. This may be of tremendous assistance during warning operations.

4. REFERENCES

Davies-Jones, R. and D. W. Burgess, 1990: Test of helicity as a tornado forecast parameter. Preprints, 16th *Conf. Severe Local Storms*, Kananaskis Park, Alberta, Canada, Amer. Meteor. Soc., 588-592.

Markowski, Paul M., E. N. Rasmussen, and J. M. Straka, 1998: The occurance of tornadoes in supercells intereacting with boundaries during VORTEX-95. *Wea. Forecasting*., **13**, 852-859.

Trapp, R. J., E. D. Mitchell, G. A. Tipton, D. W. Effertz, A. I. Watson, D. L. Andra, and M. A. Magsis, 1999: Descending and non-descending TVS signatures detected by WSR-88Ds. *Wea. Forecasting*, **14**, 625-639.

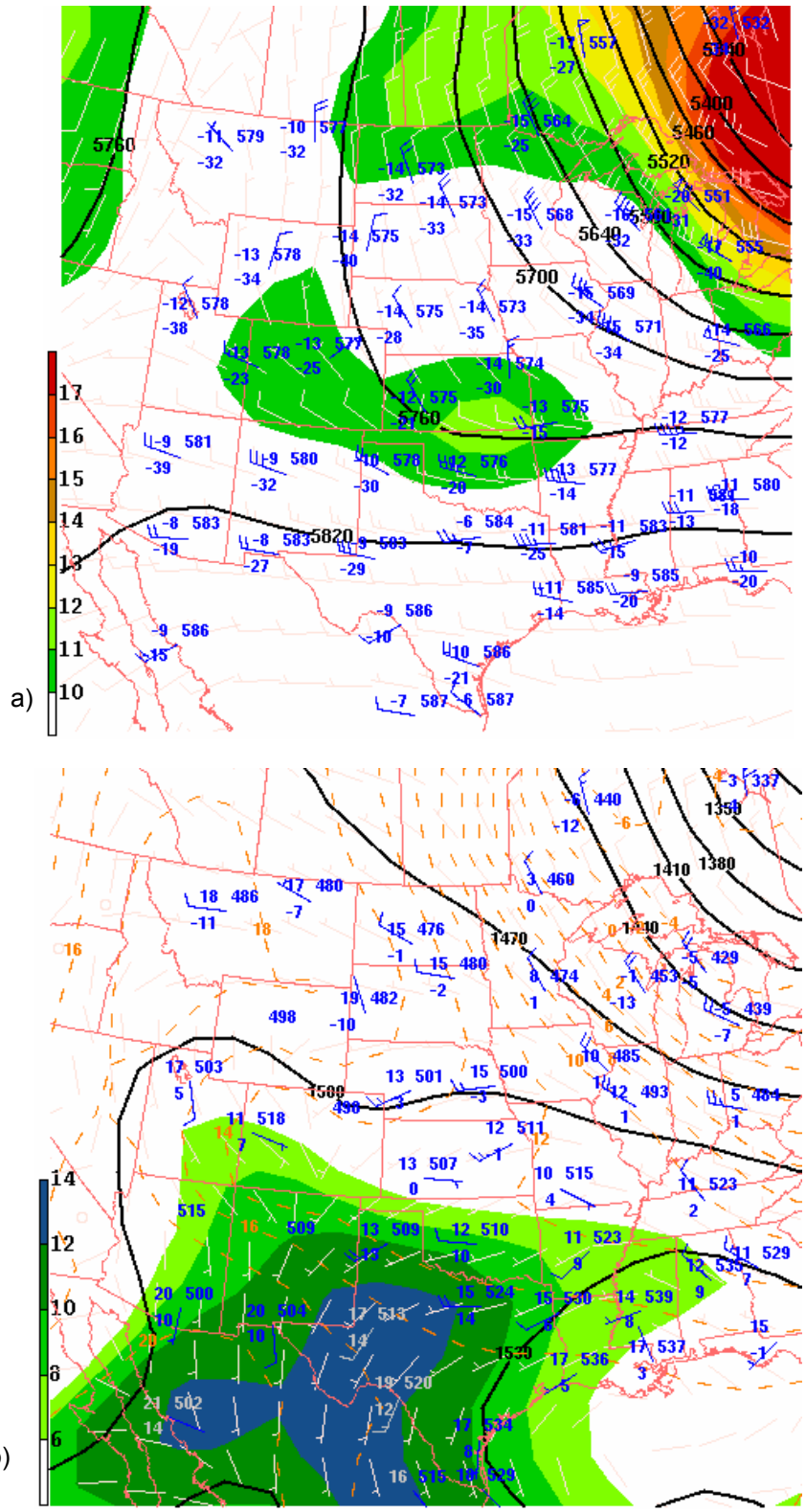

Figure 1. Objectively analyzed constant pressure maps for 5 October 2003 12 GMT at a) 500 hPa, b) 850 hPa. 500 hPa geopotential heights are contoured every 40 meters. 850 hPa heights are contoured every 30 meters. Station plot depicts the wind in knots, temperature and dewpoint in degrees Celsius, the 500 hPa heights in decameters and the 850 hPa heights in meters minus 1000. Units of absolute vorticity shading on the 500 hPa map are 10^{-5} s^{-1}. Dewpoints greater than 6 degrees Celsius are shaded on the 850 hPa map.

a)

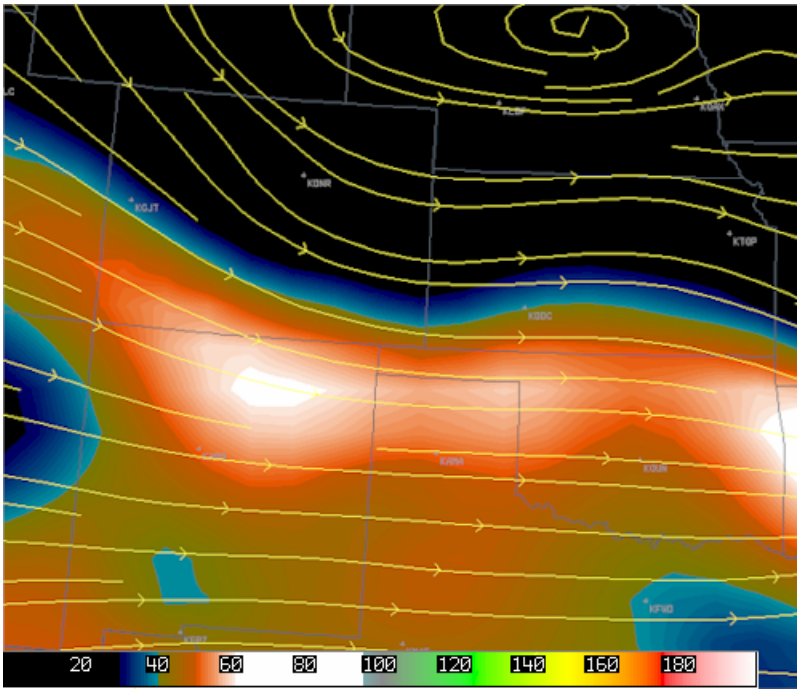

b)

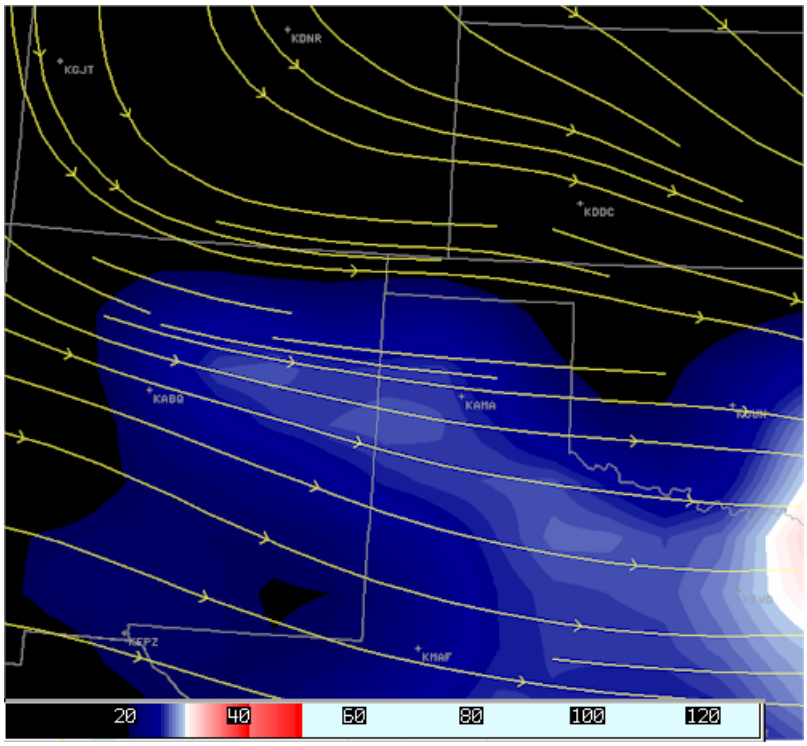

Figure 2. RUC model isotach and streamline analysis for 5 October 2003 12 GMT at a) 250 hPa and b) 500 hPa.

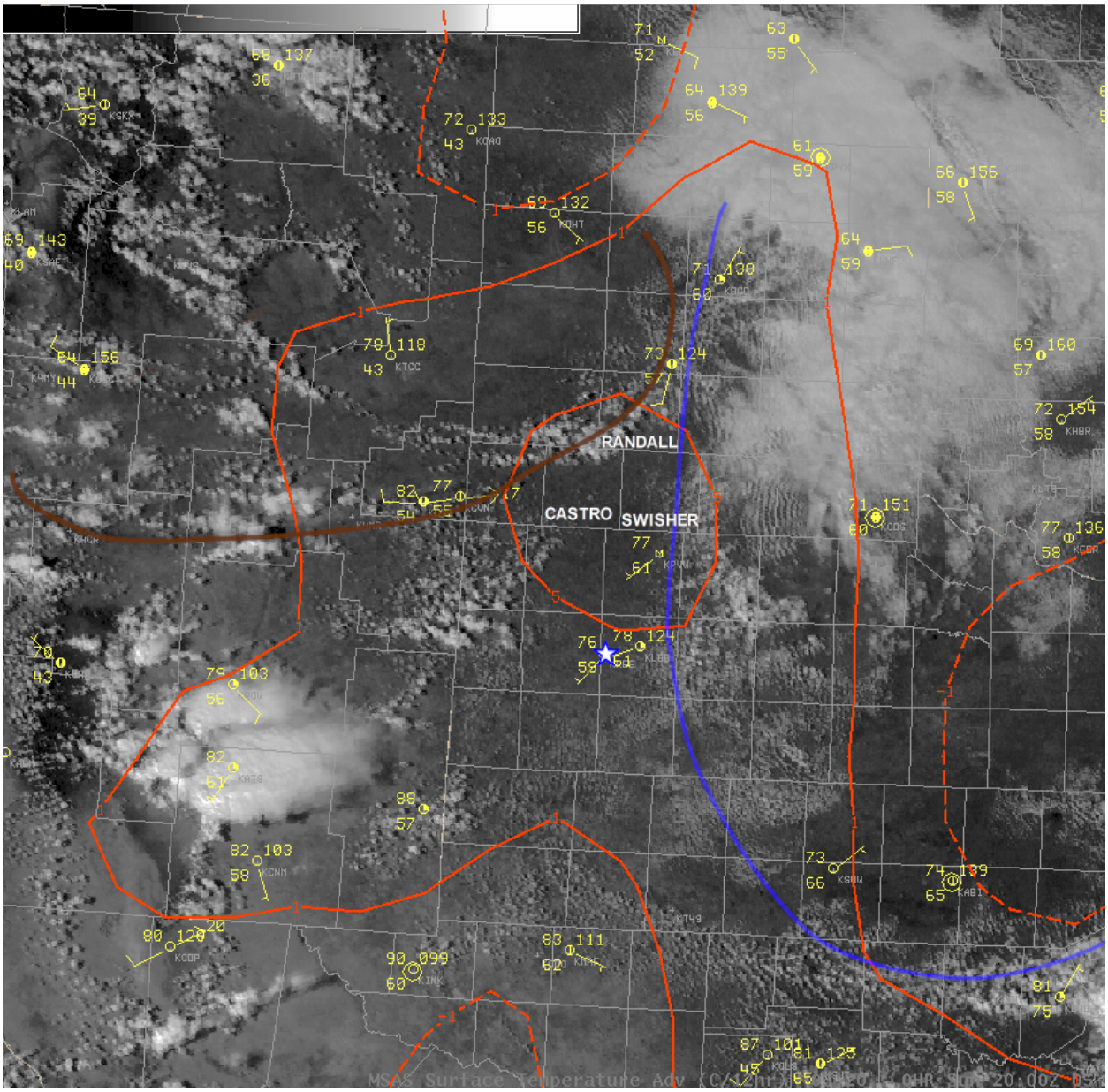

Figure 3. Visible satellite imagery for 5 October 2003 2001 GMT. Large blue line represents the outflow boundary that is moving westward on the west side while the southern extent is nearly stationary. The brown line represents a wind shift/moisture boundary advecting lower dewpoints eastward. The red lines are contours of 850 hPa temperature advection with units of degrees Celsius per 12 hours. The location of the Reese Center West Texas Mesonet site is highlighted by a white star.

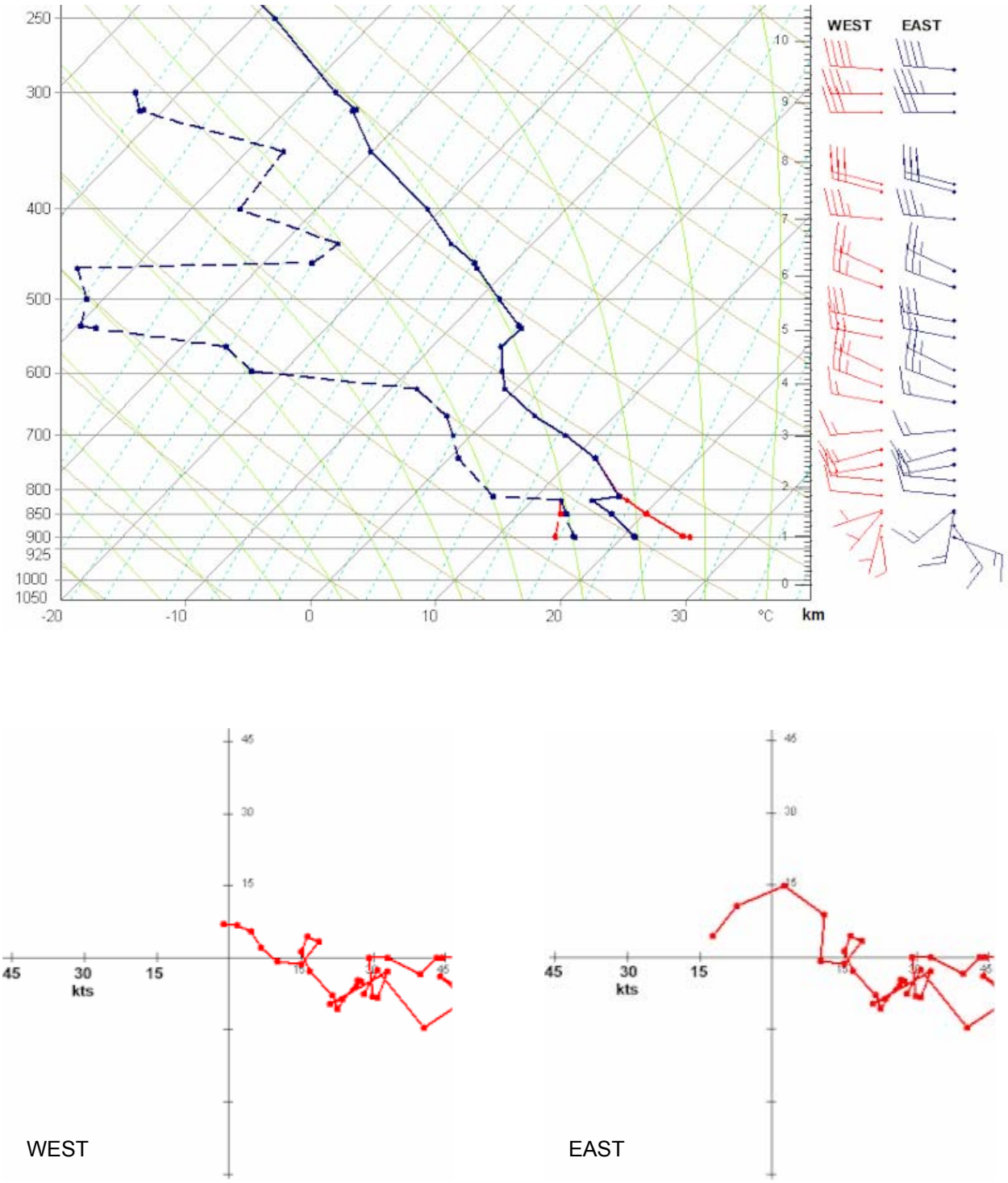

Figure 4. Surface to 250 hPa sounding from the West Texas Mesonet Reese Center site for 5 October 2003 20 GMT (position shown by the white star on the map in figure 3). The sounding has been modified with surface observations taken from mesonet sites west (red) and east (blue) of the outflow boundary. Hodographs of the wind profile are also shown.

a)

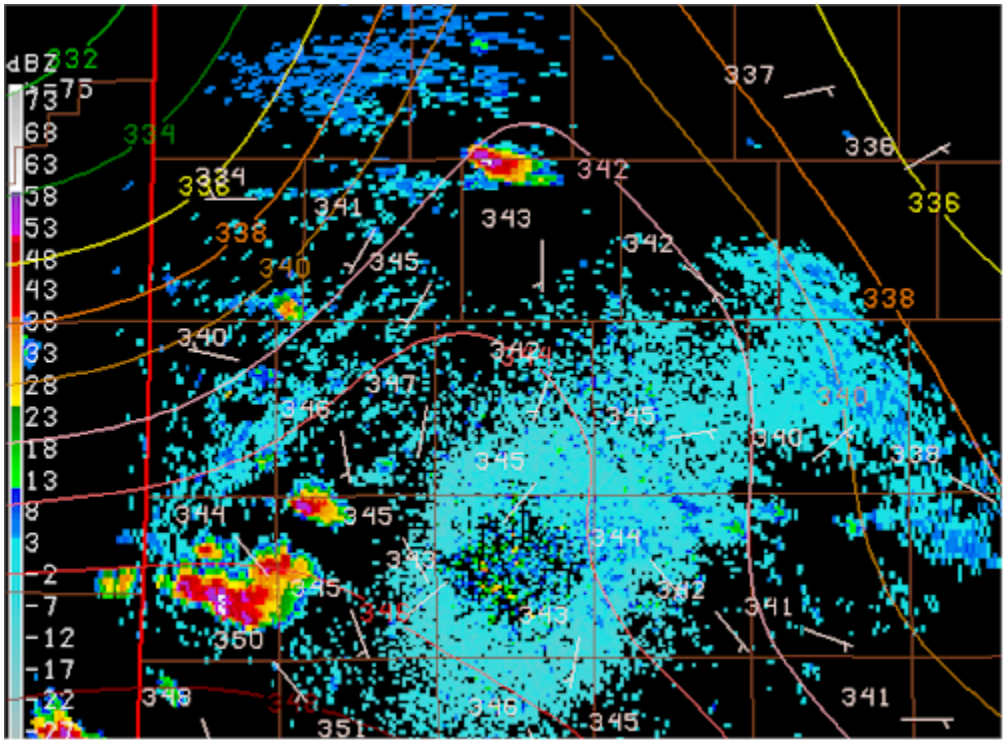

b)

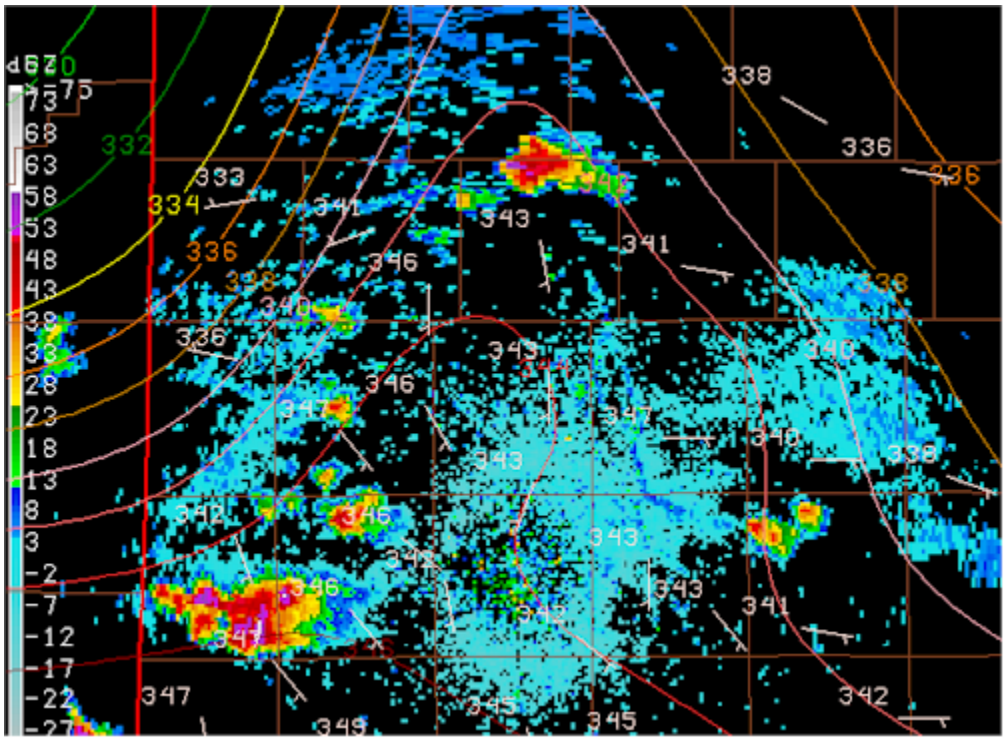

Figure 5. Gempak analysis of Theta-e (contours every 2K) overlaid on 0.5 degree Radar reflectivity for a) 2130 GMT, and b) 2200 GMT. WTXM wind observations are also shown with each full barb representing 5 m s^{-1}.

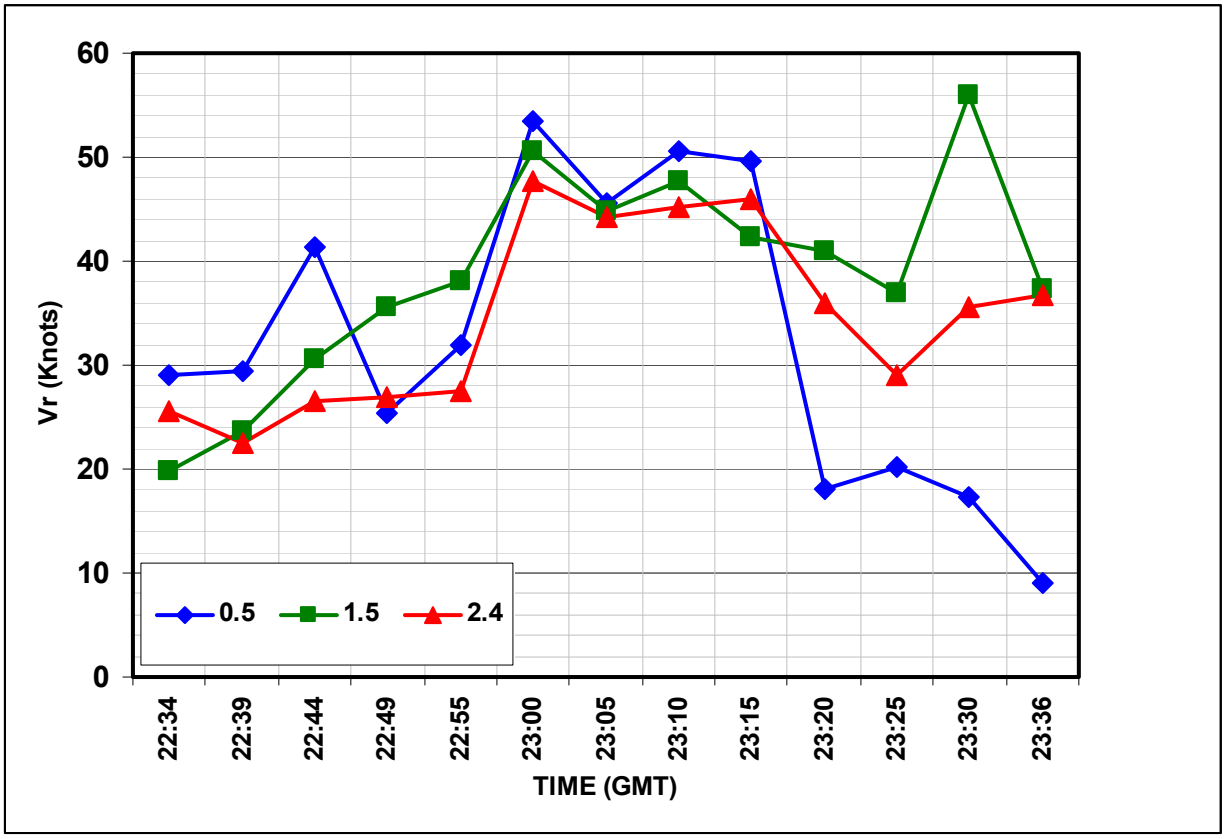

Figure 6. Graph of the rotational velocity associated with the mesocyclone for the 3 lowest elevation angles of the Lubbock WSR-88D.

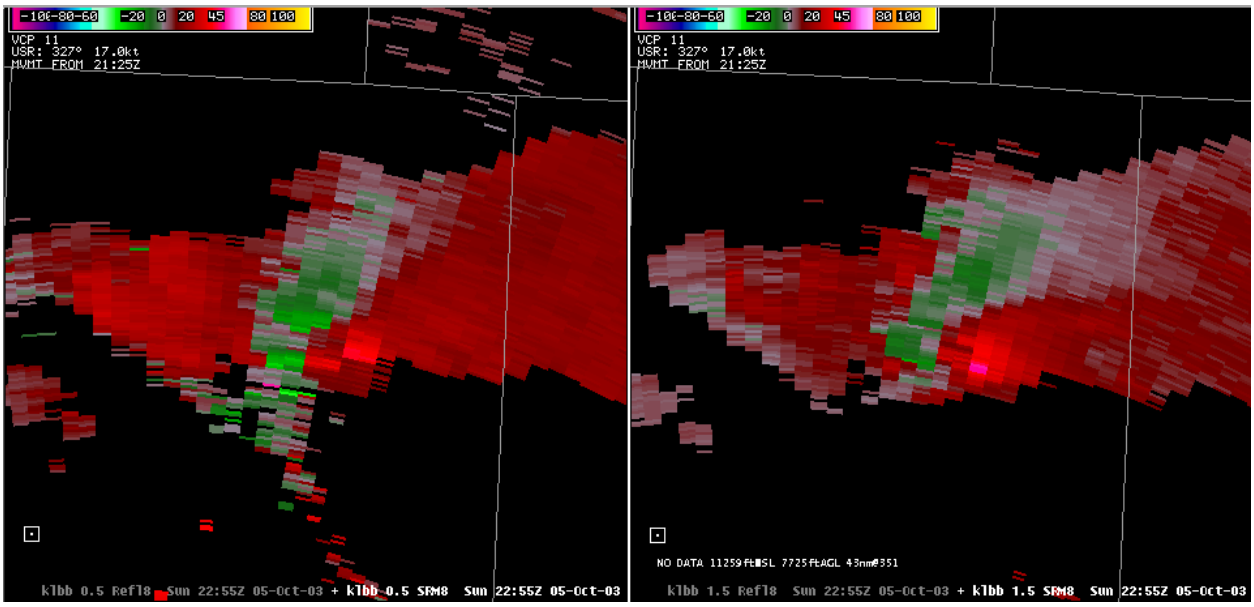

a)

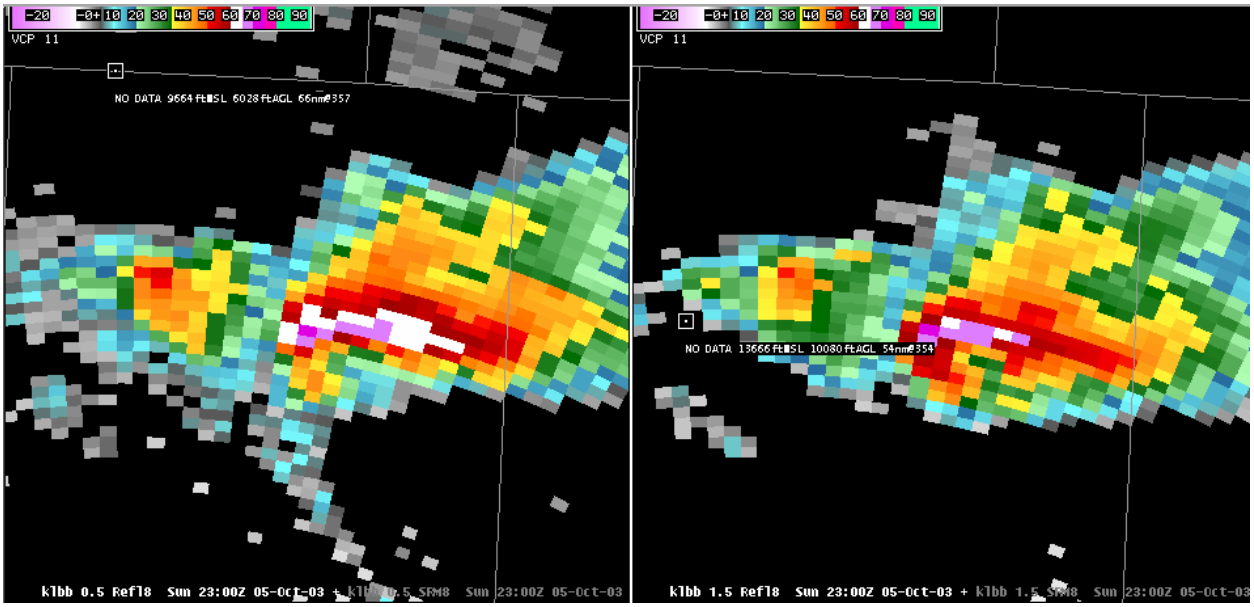

b)

Figure 7. Lubbock WSR-88D 0.5 and 1.5 elevation Radar imagery at 2300 GMT. a) Base velocity data, and b) Reflectivity data.

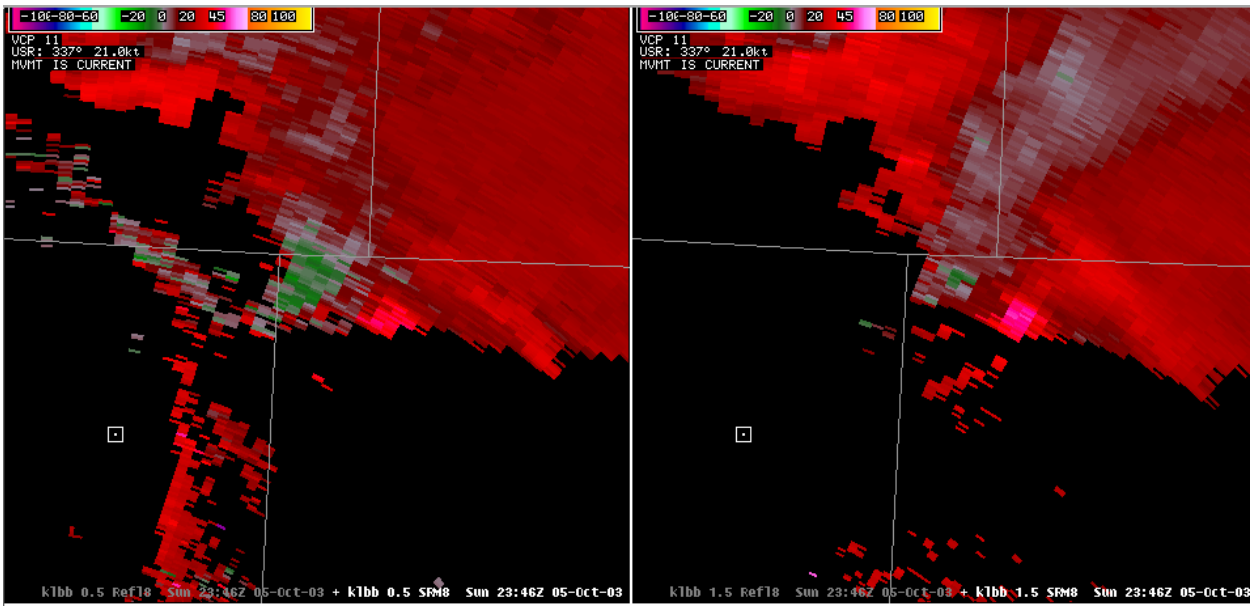

a)

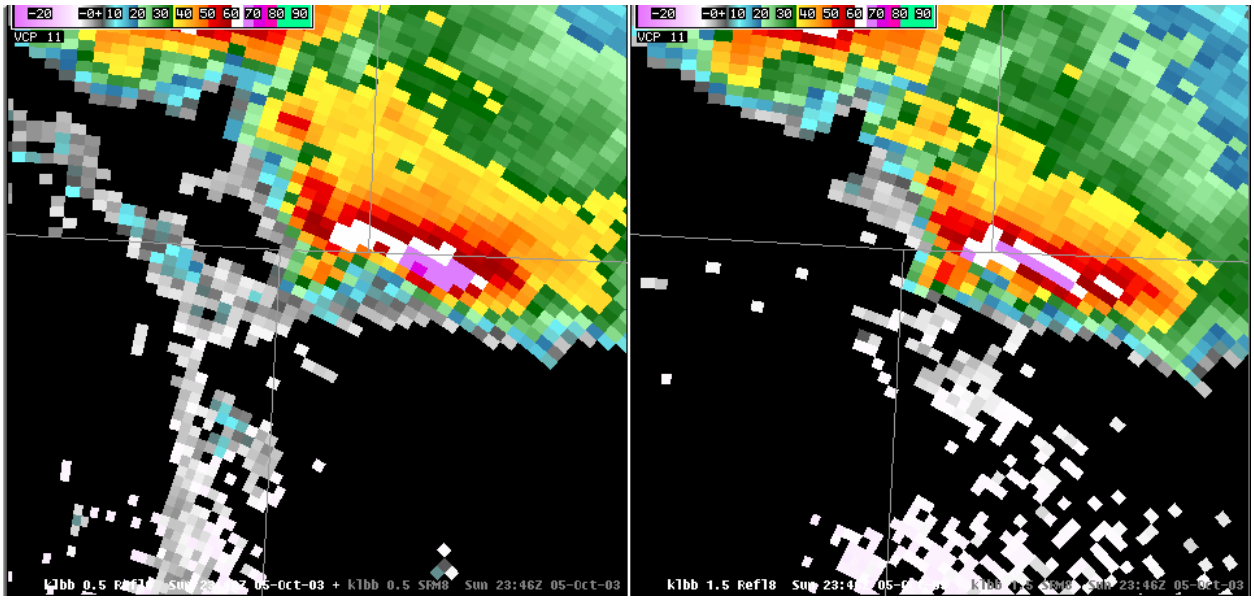

b)

Figure 8. Lubbock WSR-88D 0.5 and 1.5 elevation Radar imagery at 2346 GMT. a) Base velocity data, and b) Reflectivity data.